Optical Materials 47 (2015) 34–38

Contents lists available at ScienceDirect

Optical Materials

journal homepage: www.elsevier.com/locate/optmat

Short Communication

Polarization behaviour of femtosecond laser written waveguides in lithium niobate

M.R. Tejerina [a,b,*], D.A. Biasetti [b], G.A. Torchia [b]

[a] Facultad de Ingeniería, Universidad Nacional de La Plata, Buenos Aires, Argentina
[b] Centro de Investigaciones Ópticas de La Plata, CONICET-CIC, La Plata, Buenos Aires, Argentina

ARTICLE INFO

Article history:
Received 6 April 2015
Received in revised form 5 June 2015
Accepted 15 June 2015

ABSTRACT

In this work, we analysed the polarization of guided light in femtosecond laser written waveguides. The studied waveguides were performed with different laser pulse energies in an x-cut lithium niobate crystal. The guided intensities were experimentally measured and compared with numerical simulations reaching a qualitatively good accordance. This comparison allowed a verification of the "mechanical expansion theory" which is useful to compute the refractive index field. Also, information related to the modelling of waveguides generated with different laser pulse energies was obtained. Both of these facts are keys to design and manufacture optical circuits by using this technological approach.

Femtosecond laser machining is a relative new method widely used to fabricate optical waveguides [1,2]. These structures are very important for different technological applications like optical sensors, amplifiers and integrated lasers, among others [3]. In order to encourage an appropriate design of optical circuits (including the material selection), it is very important to know the different characteristics of this kind of waveguide: polarization of the guided light, intensity and refractive index distribution, optical losses, and so on. By analysing different works related to femtosecond laser written waveguides [4,5], it can be seen that different results were reported for the light polarizations guided in these optical confinement structures (fabricated in x-cut lithium niobate crystals): in one of the mentioned works, the authors concluded that the polarization of the guided light is only in the x-axis direction [4] and in other works, the authors measured both polarizations (x-axis and z-axis directions) [5,6].

Much effort has been made to understand the origin of these kinds of waveguides and to characterize them. In previous works [7–9], we computed the numerical parameters that emulate the mechanical expansion occurring during the interaction for a certain writing velocity and a typical energy per pulse of the laser. Also, successful results have been obtained from the comparison between numerical results and different experimental measurements, including guided light and micro-Raman mapping. In those works, we used the hypothesis that the guided region is generated by residual strain and it was assumed that only x-polarized light is guided in these waveguides. This assumption was taken from the study where the "mechanic elastic hypothesis" of the waveguide formation was presented for the first time [2]. However, the polarization behaviour of the guided light has not yet been deeply analysed.

In the present work, we examine the guided light polarization in x-cut lithium niobate written waveguides that were generated with different pulse energies of the femtosecond laser. Then, the measurements of the guided light were compared with the numerical guided modes for x- and z-polarizations and for different pulse energies. As a result, an important agreement is achieved between numerical and experimental distribution of the guided light.

The analysed waveguides were fabricated inside a congruent x-cut lithium niobate sample of $1 \times 20 \times 50$ mm dimensions. We used the femtosecond laser written technique in the transverse writing configuration to fabricate these waveguides. The sample was translated along the crystal y-direction at 25 μm/s by a Newport position stage with a resolution of 0.1 μm. The femtosecond laser was focused 250 μm below the sample surface using a 20× objective (NA = 0.4). The Ti:Zapphire ultra-fast laser with a pulse duration of 150 fs and a repetition rate of 1 KHz, was centred at a wavelength of 800 nm and polarized along the crystal z-axis direction. The energy per pulse was varied from 0.4 to 1.2 μJ (see Table 1 and Fig. 1). As it is observed from Fig. 1, different length and shapes of the modified material can be seen by optical microscopy. Each dark region is called a laser track and corresponds to the zone where the laser directly interacts with material. On both sides of these tracks, light could be guided. These waveguides have typical optical losses of about 1 dB/cm [5].

To test and characterize the fabricated waveguides, the well-known method called "end fire coupling" was carried out.

* Corresponding author at: Centro de Investigaciones Ópticas de La Plata, CONICET-CIC, La Plata, Buenos Aires, Argentina.
E-mail address: matiast@ciop.unlp.edu.ar (M.R. Tejerina).

http://dx.doi.org/10.1016/j.optmat.2015.06.030
0925-3467/

Table 1
Energy per pulse for fabricated Waveguides.

Waveguides	Energy per pulse (μJ)
#1	1.2
#2	1.0
#3	0.8
#4	0.6
#5	0.4

This method consists of launching a continuous laser at the entrance of a waveguide and collecting the near field at the output. In the implemented configuration, we used a commercial 650 nm diode laser and a set of polarizers were located before and after the waveguides to select the guided polarization acquired with a CCD camera, as shown in Fig. 2. When the polarization directions of these plates were crossed at 90°, no light was detected at the beam profiler camera. This means that the polarization of the guided light is not rotated along the waveguides.

At first, in order to compare the numerical elastic model previously developed [7] with the current guiding structures, the experimental guided modes were fitted with those obtained from simulations. We computed with the mentioned numerical tool the expected guided light for *x*-axis and *z*-axis polarizations and for different mechanical expansions. In the numerical model, a static mechanical expansion of an ellipse is set in an elastic domain. This model has four parameters: two associated with the ellipse geometry (a and b) and two associated with the horizontal and vertical expansion magnitude (α and β) [7]. After setting an expansion, the strain field in the surrounding area of the ellipse is retrieved (by using the Finite Element Method) and used, through the corresponding piezo-optical properties, to compute the refractive index field. Then, by solving the Variational Formulation of the scalar Helmholtz equation with the Finite Element Method [10], the guided modes were obtained. The values of the lithium niobate elastic and piezo-optic constants that were set in this modelling are presented in Table 2 [11]. The mechanical expansion set in the numerical model was considered along the *z*-axis direction ($\beta = 0$), as determined in a previous work [8] for this kind of

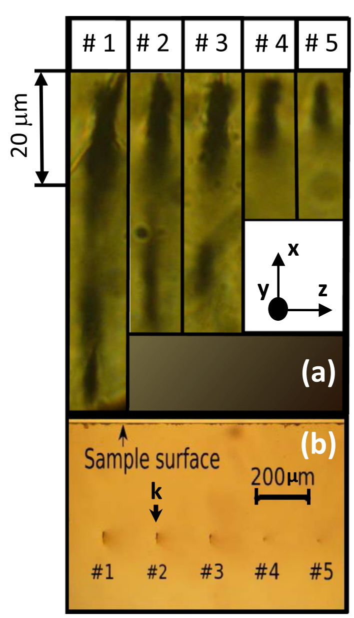

Fig. 1. Images taken by an optical microscope of the performed laser tracks: (a) detailed images and (b) an overall image, the *k*-direction indicates the incidence of the writing laser.

waveguide. The different intensity distributions of the computed guided modes (i.e. those computed modes which the effective refractive index value was greater than the substrate refractive index value and less than the maximum refractive index of the waveguide) were summed and plotted to contrast them with the experimentally acquired guided modes.

As mentioned above, the origin of the guided polarization in femtosecond laser written waveguides in lithium niobate, is not yet completely understood. Taking into account that the guided polarization is an important characteristic of a guiding structure, in this paper we analysed this characteristic in waveguides fabricated with different energies per pulse in the mentioned crystal.

In the studied waveguides, the *x*-polarization guided modes are more spatially confined than the *z*-polarization guided modes. Fig. 3 shows the experimentally guided modes at both sides of the performed laser tracks and for both polarizations (*z*- and *x*-axis). The guided intensities for the two different polarizations have different spatial distribution and generally, the guided intensity is approximately symmetric with respect to each laser track. These facts are in agreement with observations reported in a previous work [6].

Regarding the *x*-polarized light, the guided modes in the different Waveguides (from #1 to #5) have, in general, different spatial distributions; in Waveguides #1, four lobes can be seen and the area that occupies the guided intensity is larger than the area occupied by that measured in the other Waveguides (from #2 to #5). Also, in the surrounding areas of Track #1, less confined guided light can be seen in the lower region near a "secondary laser track"; these "secondary modes" are also observed in the surrounding areas of Track #2 and #3, decreasing their optical confinement. This secondary laser track is originated by a non-linear propagation of the laser writing beam [2]. In Waveguides #2 and #3, the main guided intensity has three well defined lobes and an evanescent fourth lobe with different geometries: in Waveguides #2, the guided modes in the main region seem to be considerably modified by the corresponding secondary guided region situated below it. In Waveguides #4, three aligned lobes are also observed but less spatially confined than in Waveguides #1, #2 and #3. In Waveguides #5, only two lobes can be observed. Generally, these lobes are approximately aligned.

On the other hand, when considering the *z*-polarized guided light; this is generally less spatially confined than the *x*-polarized light: the different modes are extended in an evanescent way around the laser tracks. Also, as it can be seen in Waveguides #1 to #3 (in Fig. 3) the spatial confinement of the z-polarized guided light is almost constant and for Waveguides #4 and #5, it is considerably reduced.

In order to match the described experimental results (guided intensities) with those obtained from the numerical model, several iterations of the numerical expansion were performed starting with the parameters values (a, b, α, β) obtained in a previous work [7]. Then, different numerical expansions (several a and b values) were computed and their results were compared with the experimental results of the *x*-polarized guided light (which shows a more defined spatial distribution than the *z*-polarized light). From this iterative process, the geometrical parameters $a = 3$ μm and $b = 4$ μm were defined suitable for Waveguides #3, #4 and #5. The numerically guided modes did not match those observed experimentally for other values of a and b with significant differences (around a 10%) when compared to the defined values. After setting a and b values, we tested several α values and assigned an expansion parameter value to each pair of the mentioned Waveguides (#3, #4 and #5), as presented in Table 3. Fig. 4 shows the experimental and simulated propagation modes corresponding to Waveguides #3, #4 and #5. It can be seen that the experimentally guided modes in the mentioned waveguides present an

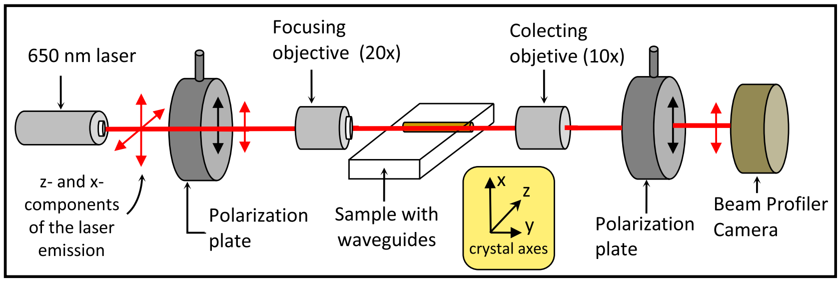

Fig. 2. Scheme of the "end fire" method setup used to couple light and to select the guided light polarization.

Table 2
Elements of the compliance matrix (C_{ij}) and piezo-optic constants (p_{ij}) of lithium niobate used in simulations.

C_{ij} (GPa)	C_{11} = 205	C_{12} = 57	C_{13} = 70	C_{14} = 7.9	C_{33} = 249	C_{44} = 60.9	C_{66} = 75	–
p_{ij} (Adimensional)	p_{11} = −0.026	p_{12} = 0.09	p_{13} = 0.133	p_{14} = −0.075	p_{31} = 0.179	p_{33} = 0.071	p_{41} = −0.151	p_{44} = 0.146

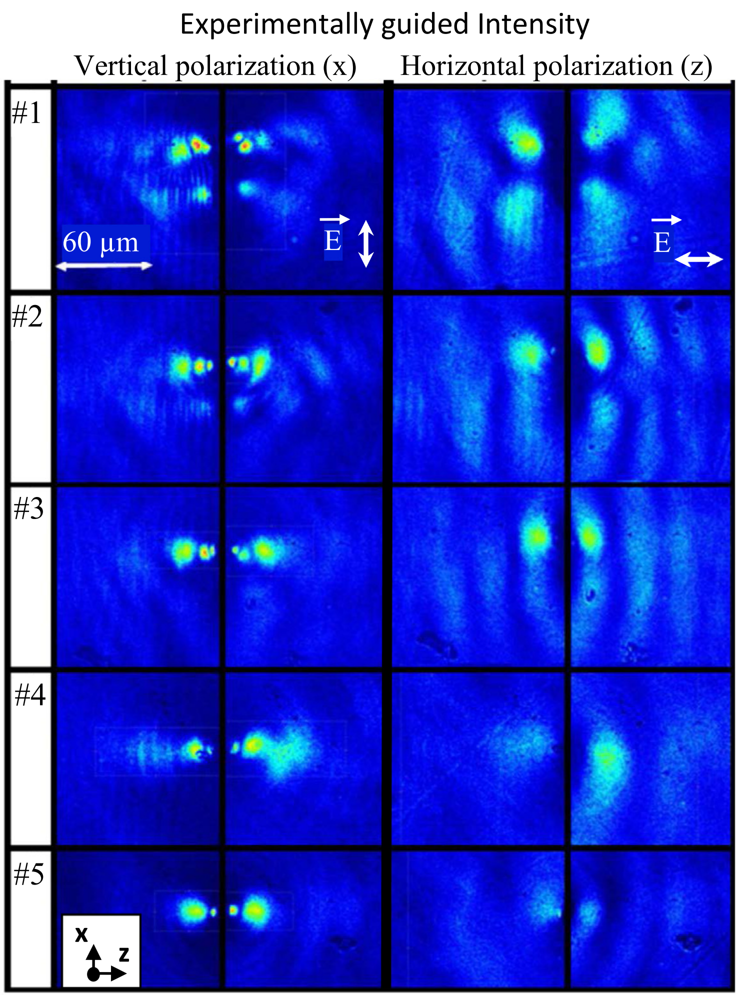

Fig. 3. Experimentally guided light profile in the different waveguides for x- and z-polarization. All the images have the same spatial scale.

Table 3
The different waveguides and assigned expansion parameters of the model.

Track/Waveguides	#3	#4	#5
e_p (µJ)	0.8	0.6	0.4
α	0.008	0.005	0.003
β	0	0	0

important accordance with the numerically obtained modes. Particularly, the best agreement was obtained for guiding structure #5 and for the x-polarized guided light. Subsequently, for guiding structures #4 and #3, although less accordance was obtained, the numerical results qualitatively matched the acquired guided intensities for this polarization.

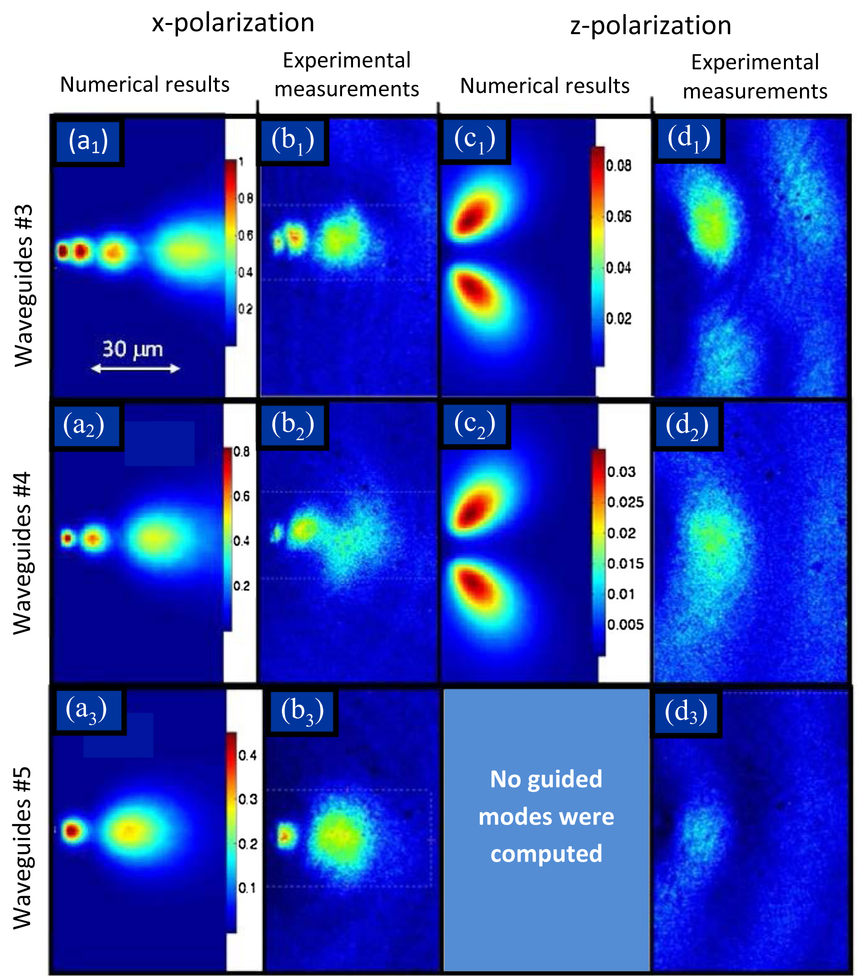

Fig. 4. Numerically computed and experimentally measured intensity distributions for *x*- and *z*-axis polarization. All the images have the same spatial scale.

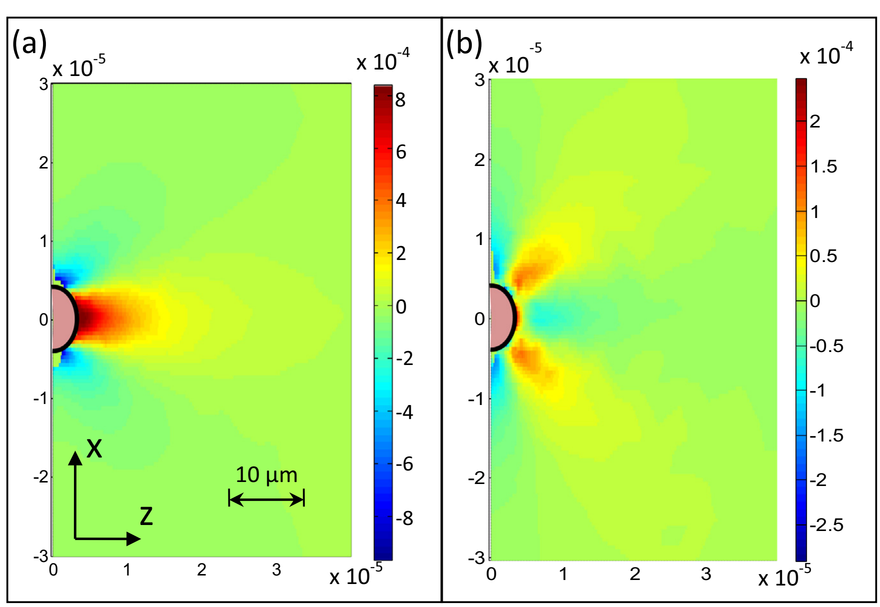

Fig. 5. (a) Δn_x field assigned to Waveguides #5, (b) Δn_z field assigned to Waveguides #5. Inside the half-ellipse the refractive index variation was assumed equal to -1×10^{-2} for both polarizations.

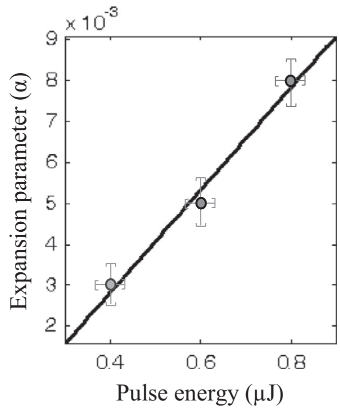

Fig. 6. Expansion parameter (α) vs. pulse energy (μJ). The solid line is a linear fitting of data.

From the above results, the Δn_x field that was computed with the numerical model and associated to Waveguides #5 is shown in Fig. 5(a). The Δn_x corresponding to the waveguides #4 and #3 are proportional to this map. For them, the maximum index increment is 1.3×10^{-3} and 2.3×10^{-3}, respectively.

On the other hand, for the z-axis polarization, less accordance can be seen when comparing the computed intensity with the experimental measurements. This difference can be generated by dynamic or visco-plastic effects during the laser processing. The Δn_z field computed with the numerical model and assigned to Waveguides #5 is shown in Fig. 5(b). The Δn_z field corresponding to Waveguides #4 and #3 are proportional to this map. For these, the maximum index variation is 4.1×10^{-4} and 6.6×10^{-4}, respectively.

In contrast, for Waveguides #1 and #2, the elastic numerical model could not match the experimental results. This is because the waveguides generated with a higher energy per pulse shows considerably structural modifications, including a secondary modification in the material due to a nonlinear propagation of the writing beam [5,2]. This alters the main guided region. In this regimen of the interaction, as is mentioned in other works [3], the static-elastic numerical model clearly does not follow the material behaviour.

Finally, in order to quantify this waveguide writing effect for the mentioned experimental set-up, the obtained α expansion parameter vs. the pulse energy of the writing beam is plotted in Fig. 6. It can be seen that when the pulse energy is increased, α must also increase to match the experimental intensity distribution and, the slope of this dependence is equal to $2.5 \pm 0.1 \times 10^{-3}$ 1/μJ. This information is relevant to simulate and so, design different optical circuits written using energies of femtosecond laser pulses up to 0.8 μJ.

In this work, we presented an analysis of the polarized light guided in waveguides that were fabricated with different energy pulses using a typical femtosecond laser in an x-cut lithium niobate crystal. The different guided intensities were acquired experimentally and fitted with a finite element numerical model. A qualitatively good accordance was reached for most of the studied waveguides. From this comparison, we concluded that the elastic model, at least partly, explains the polarization behaviour of the guided light in the studied waveguides. Furthermore, we obtained empirical data which relates the energy per pulse of the femtosecond laser with the numerical expansion parameters of the model. This information is useful to simulate and design optical circuits embedded in lithium niobate crystals for technological applications. In future works, we expect to include visco-plastic/dynamic effects in the numerical simulations and compare the behaviour of different lithium niobate crystal orientations as well as other bulk materials.

Acknowledgment

This work was partially supported by Agencia de Promoción Científica y Tecnológica (Argentina) under project PICT-2010-2575 and by CONICET (Argentina) under project PIP 5934.

The authors want to thank Eng. Christopher Young (Facultad de Ingeniería, Universidad Nacional de La Plata, Argentina) for his valuable language/linguistic revision.

References

[1] G. Marowsky (Ed.), Planar Waveguides and other Confined Geometries: Theory, Technology, Production and Novel Applications, Springer, USA, 2014.
[2] R. Osellame, G. Cerullo, R. Ramponi (Eds.), Femtosecond laser micromachining, Springer-Verlag, Berlin, 2012.
[3] G. Lifante, Integrated Photonics: Fundamentals, Wiley, England, 2007.
[4] J. Burghoff, S. Nolte, A. Tünnermann, Appl. Phys. A 89 (2007) 127–132.
[5] A. Ródenas, L.M. Maestro, M.O. Ramirez, G.A. Torchia, L. Roso, F. Chen, D. Jaque, J. Appl. Phys. 106 (2009) 0131101–131106.
[6] J. Burghoff, H. Hartung, S. Nolte, A. Tünnermann, Appl. Phys. A 86 (2006) 165–170.
[7] M. Tejerina, G.A. Torchia, Appl. Phys. A 110 (2012) 591–594.
[8] M.R. Tejerina, D. Jaque, G.A. Torchia, Opt. Mater. 36 (2014) 936–940.
[9] M.R. Tejerina, PhD Thesis Caracterización de guías de onda ópticas generadas con láser de femtosegundos en niobato de litio, Universidad Nacional de La Plata, 2014, <http://hdl.handle.net/10915/40074>.
[10] K. Okamoto, Fundamentals of Optical Waveguides, Elsevier, USA, 2006.
[11] I. Tomeno, S. Matsumura, C. Florea, in: K.K. Wong (Ed.), Properties of Lithium Niobate, INSPEC, IEE (The Institution of Electrical Engineers), United Kingdom, 2002, pp. 57 (Chapter 4.1 and 4.2).